NANO-ELECTROMECHANICAL ZERO-DIMENSIONAL FREESTANDING NANOGAP ACTUATOR

Jun Hyun Han[1], Norimasa Yoshimizu[2], Tiffany Cheng[2], Michael Ziwisky[1], Sunil A. Bhave[2], Amit Lal[2], and Chung Hoon Lee[1]

[1]Marquette University, Milwaukee, Wisconsin, USA

[2]Cornell University, Ithaca, New York, USA

ABSTRACT

Micromachined free standing nanogap with metal electrodes is presented. The gap size is as small as 17 nm, and can be reduced further with electrostatic or piezoelectric actuation. The nanoscale gap is fabricated by industrial standard optical lithography and anisotropic wet chemical Si etching. Electron transport between the metal electrodes with optical stimulus enhancing photon-electron coupling (plasmon) is presented.

INTRODUCTION

Metal nanogap capacitors are potentially important components for nanoscale electronic sensors and electronics. Nanogap electrodes, made of conductive organics or metals, have been used for molecular electronics [1], optical plasmonics [2,3], tunneling based sensors [4], and bio/chemical sensors [5,6]. A key attribute of high performance nanogap devices is the ability to minimize the tip size and position, and at the same time control the nanoscale gap size precisely. Previous attempts to form nanogaps have been made by moving two tips mounted on macroscopic actuators close together, which prevents high-bandwidth gap control. Various methods of conductive nanogap nanofabrication have been developed: mostly direct electron-beam lithography [7], mechanical pulling [8], shadow masking [9], electromigration [10], electroplating [11], focused ion beam (FIB) [12], angled metal evaporation [13], and silicon micromachining [3,14,15]. Most nanogaps are fabricated by laborious serial processes that would introduce a large variation in gap sizes or on a substrate that would interfere with electrical and optical measurements. Recently, a microfabricated plasmon converter was made [3], but the gap size was initially large (a few micrometers) and it required large forces to actuate. It also lacks the very sharp tips necessary for tunneling and plasmon confinement.

In this paper, we present results on the development of a nanogap actuator that effectively creates a zero-dimensional gap that can control the field emission and a plasmon within the gap. Figure 1 shows the device consisting of two arms with nanoscale sharp tips and an electrostatic actuator. The nanogaps are fabricated by conventional optical lithography and anisotropic wet chemical silicon etching with unique double-layer etch mask processes. These processes produce highly symmetric and reproducible nanoscale gaps as small as a few tens of nanometers formed by atomically sharp tips facing each other. This process flow does NOT require e-beam lithography, enabling conventional foundries to fabricate devices.

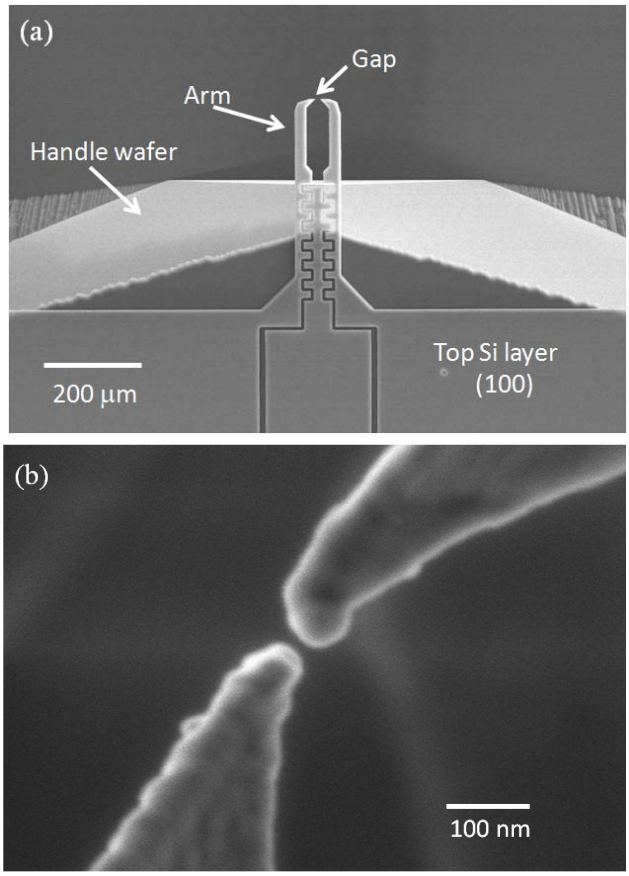

Figure 1. Free-standing nanogap on an SOI wafer. (a) Overview of nanogap device. The top Si layer is physically and electrically isolated from the handle wafer by buried oxide. (b) Close-up of the ~17 nm gap formed by atomically sharp tips.

The nanogaps, which are on the order of tens of nm, are fabricated on the top silicon layer of an SOI wafer, and isolated from the handle wafer by undercutting a buried oxide (3 μm thick) in HF solution, which allows a metallization of the entire device with flood metal evaporation. The metal will serve as electrodes for electrical/optical measurements of the nanogaps. Electrical characterization of the nanogaps in vacuum has been performed with DC bias voltages across the nanogap, measuring tunneling current with and without optical stimulation by a laser. Electron transport through the nanogap with a DC bias across the metal coated tips can be

characterized by Fowler-Nordheim (F-N) tunneling current, which is a function of the metal work function, surface conditions of electrodes, the gap size, and the radius of curvature of the tips. The fabrication process is novel in the sense that any metal layer can be deposited on the nanogap. The metal layer serves for electrical and chemical functions such as molecular binding and catalysts. With a spring constant of 40 N/m, the gap can be controlled with nanoscale precision with a few volts of actuation voltage.

DEVICE FABRICATION

The fabrication of the nanogap starts from an SOI wafer, (100) orientation, 5 µm thick top Si layer, 3 µm thick buried silicon dioxide (SiO_2), and 600 µm thick handle wafer. Thermal SiO_2 (250 nm) and low stress SiN (300 nm) films are grown and deposited on the SOI wafer in sequence. The fabrication of the devices is performed by two sequential steps of anisotropic wet chemical (potassium hydroxide, KOH, in this work) and Deep RIE Si etchings. The two thin films serve as etch masks in subsequent fabrication processes.

The first optical patterning on the top SiN film determines all of the dimensions of the highly symmetrical nanogap devices as shown in Figure 2 (a). The pattern is aligned along the [100] direction of Si crystal, which is 45° rotated with respect to the major flat of (100) Si wafer. The SiN film is etched by Reactive Ion Etching (RIE) with CF_4 gas. The patterned SiN film serves as the etch mask for KOH Si etching throughout the rest of the fabrication process. After the SiN patterning and etching, the initially grown SiO_2 film is exposed. The selected SiO_2 is patterned and etched by buffered oxide etchant (BOE). This process step defines the one side of the gap bounded by (111) planes and inner sides of the arms as shown in Figure 2 (b). A second SiO_2 film is thermally grown to cover the etched surfaces. The area indicated as *A* in Figure 2 (b) is patterned and etched to expose the top Si. The second KOH Si etch forms the gap and arms as shown in Figure 2 (c). The KOH etched surfaces of the arms are {100} planes, which are vertical to the top Si surface, (100) plane, resulting in a well defined cantilever profile for actuation. The final fabrication step of the device is a DRIE process forming an electrostatic actuator as shown in Figure 2 (c). The fabricated nanogap device is shown in Figure 2 (d).

The gap size made using this method shown in Figure 2 is 17 nm without actuation. After the device fabrication, the buried oxide is etched with HF. This SiO_2 undercut releases the nanogap and arms from the substrate and frees them to move when actuated by electrostatic or piezoelectric actuation. The SiO_2 undercut will make the top Si layer electrically isolated from the handle wafer when a flood metal evaporation is done on the device as shown in Figure 3. The leakage current between the metal layer on the top Si layer and handle wafer is around 100 femtoamps (fA) at 20 V bias indicating effective electrical isolation. The metal will serve as electrodes for electrical/optical measurements of the nanogaps.

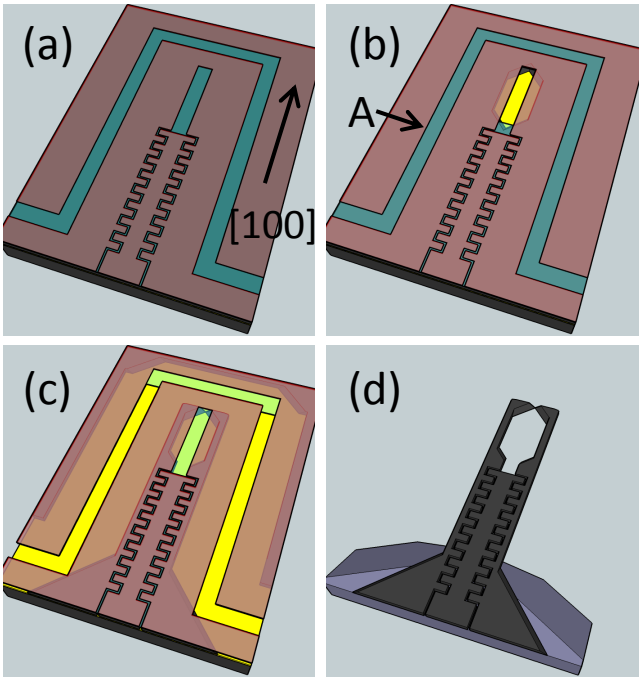

Figure 2. Fabrication processes. (a) Patterning SiN film for all parts at once. The pattern is aligned along the [100] direction. (b) Selective etch (KOH) for the inside arms followed by DRIE for electrostatic actuator. The wafer is oxidized to protect the etched surface for next process (c) KOH for the gap and arms formation (d) device release.

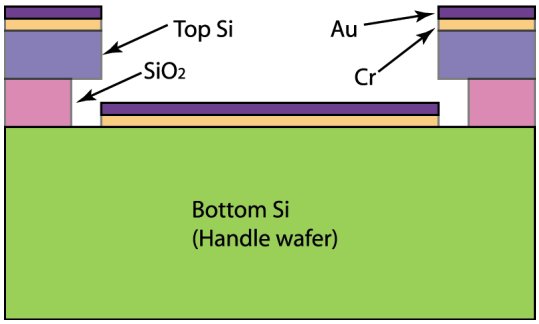

Figure 3. Cross-sectional view of the device showing the electrical isolation of metal layers on top Si layer and the handle wafer. No masking or lithography is required for the flood metallization.

DEVICE ACTUATION

Two actuation methods, electrostatic and piezoelectric, are used to further reduce the gap size. ANSYS modal analysis is used to find the resonance frequency of the arm as shown in Figure 4. The modal analysis also shows the lateral motion of the arm. For the piezoelectric actuation, the nanogap device is mounted on a PZT plate (5 mm by 10 mm and 0.5 mm thick) with adhesive epoxy. AC voltage is applied to the PZT plate inducing ultrasonic vibration to the device. Measured resonance frequency of the arm and the displacement of the tip are shown in Figure 5. For the electrostatic actuation, AC voltage from a function generator is applied to the electrodes on the device,

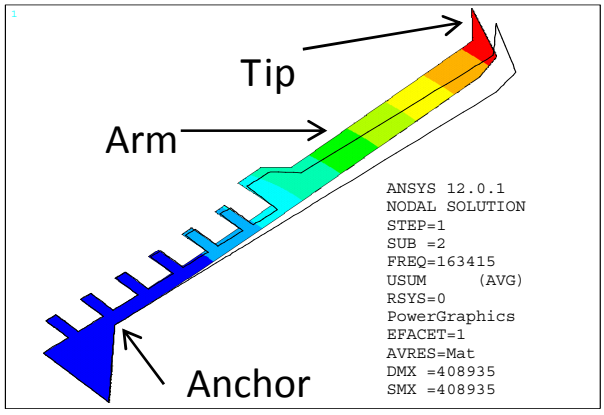

Figure 4. ANSYS analysis for vibrational modes. It shows lateral motion of arm at the resonance frequency of 163 kHz.

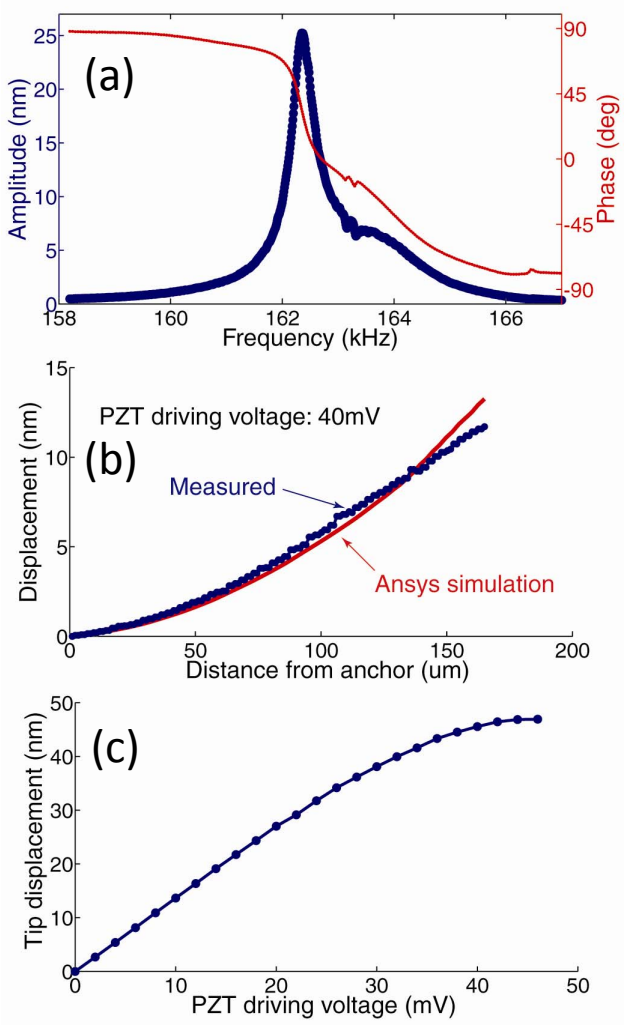

Figure 5. Mechanical characteristics of the nanogap. A PZT plate is adhesively bonded to the back of the handle wafer,and actuates the arms to control the gap size. (a) Resonance frequency of arms. The quality factor (Q) is about 300 in air. (b) Displacement profile of the arm from anchor to tip. (c) Measured tip displacement as a function of PZT driving voltage.

which is connected to the comb drive. A 5V AC bias across the arms at their resonance frequency (120 kHz) results in 8 nm maximum displacement of the tip. With both actuation methods, the gap can be reduced from the average size of tens of nanometers to a few nanometers.

TUNNELING CURRENT

Tunneling current between two electrodes can be analyzed with the Fowler-Nordheim (F-N) equation,

$$I = B\phi^{-1}\beta^2 V^2 \exp\left[-C\phi^{3/2}/\beta V\right] \qquad (1)$$

where B and C are constants, V is the applied voltage, ϕ is the work function of the emitter material, and β is the field enhancement factor of emitter structure. The tunneling current is exponentially proportional to the work function of a metal. The tunneling current is a function of the radius of curvature of the tip and size of the gap (which affects the electric field strength).

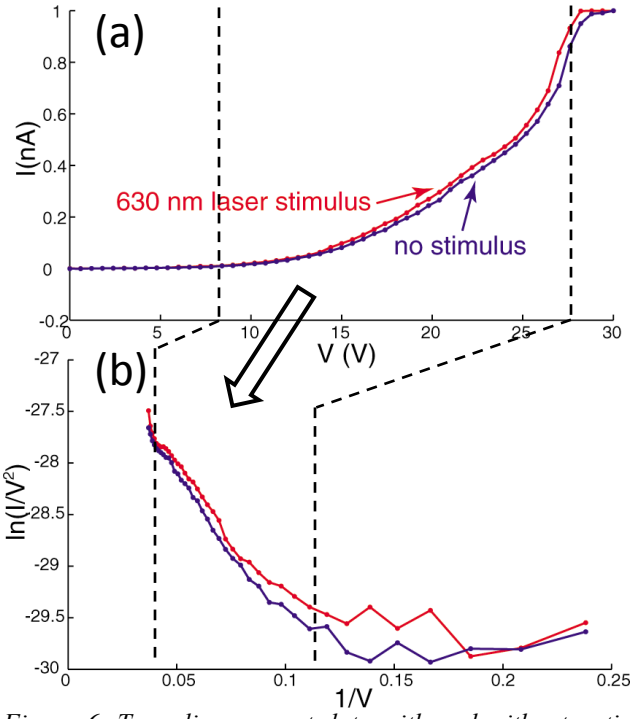

Figure 6. Tunneling current data with and without optical stimulation on gap. (a) Tunneling current through the gap with the bias voltage of 30 V (b) F-N plot showing a linear relation Ln[I/V^2] and 1/V.

In addition to the physical parameters, the metal surface can be modified with molecules and other materials affecting the electron transport in the gap. Because the tunneling current is very sensitive to the work function, monitoring the tunneling current could be used as a chemical or bio sensor with molecular level sensitivity. The characteristic of F-N tunneling current is a linear relation between *Ln[I/V^2]* and *1/V*. Figure 6 (a) shows the tunneling current through the gap with and without laser light.

As shown in Figure 6 (b), the electrical current through the gap follows F-N tunneling characteristics with and without laser light. The measured current, on the order of nanoamps, is as expected for the nanogap dimensions. When more than 40 nA flows through the nanogap, the metal layer on the tips is damaged. The metal layers used in this work are Au/Cr layers, and the tip radius of curvature is ~30 nm.

Once exposed to incident laser beam, with its THz frequency electromagnetic modulation at the nanogap, plasmons can be formed owing to the carrier densities in the nanogap electrodes. As seen in Figure 6, the optical stimulus (5 mW laser, 630 nm wavelength, not focused) on the gap increases the current. The increase in the current can be explained by the field enhancement (plasmon) within the nanogap lowering the emission threshold due to displacement charge. Efficient photon coupling can occur when the incident photon can drive charges to the metallic gap [2,16]. Our nanogap is coated with Au to optimize the photon coupling. Gold has a large magnitude index of refraction in the optical spectrum, and is an appropriate metal to enhance photon-electron coupling [16]. Combined with resonant actuation, we can measure the plasmon effect with a much higher S/N ratio by sampling at the resonant frequency.

SUMMARY

Wafer-scale nanogap devices are fabricated with conventional optical lithography and anisotropic wet chemical Si etching. Highly symmetrical nanogaps as small as 17 nm are fabricated with unique double-layer (SiN/SiO2) etch masking technique. With electrostatic or piezoelectric actuations, the size of the nanogap can be further reduced for applications requiring extremely narrow gaps. Electrical characteristics of the gap with and without optical stimulus have been analyzed with F-N analysis. Optical stimulation of the gap has shown the effect of plasmon on the electrical transport. Our nanogap device can potentially be used as a platform for chemical/biological sensors owing to the fact that any metal layer (serving electrical and chemical functions such as molecular binding or catalysts) can be deposited on the arms forming the nanogap.

REFERENCES

[1] D. R. Strachan, D. E. Smith, D. E. Johnston, T.-H. Park, M. J. Therien, D. A. Bonnell, and A. T. Johnson, "Controlled fabrication of nanogaps in ambient environment for molecular electronics," *Appl. Phys. Lett.*, vol. 86, p. 043109, 2005.

[2] D. P. Fromm, A. Sundaramurthy, P. J. Schuck, G. Kino, and W. E. Moerner, "Gap-dependent optical coupling of single "bowtie" nanoantennas resonant in the visible," *Nano Lett.*, vol. 4, no. 5, pp. 957–961, 2004.

[3] K. Iwami, T. Ono, and M. Esashi, "Optical near-field probe integrated with self-aligned bow-tie antenna and electrostatic actuator for local field enhancement," *Microelectromechanical Systems, Journal of*, vol. 15, no. 5, pp. 1201 –1208, 2006.

[4] A. Partridge, J. Reynolds, J. Grade, B. Kane, N. Maluf, G. Kovacs, and T. Kenny, "An integrated controller for tunnel sensors," *Solid-State Circuits, IEEE Journal of*, vol. 34, no. 8, pp. 1099 –1107, 1999.

[5] M. Yi, K.-H. Jeong, and L. P. Lee, "Theoretical and experimental study towards a nanogap dielectric biosensor," *Biosensors and Bioelectronics*, vol. 20, no. 7, pp. 1320–1326, 2005.

[6] C. S. Ah, Y. J. Yun, J. S. Lee, H. J. Park, D. H. Ha, and W. S. Yun, "Fabrication of integrated nanogap electrodes by surface-catalyzed chemical deposition," *Appl. Phys. Lett.*, vol. 88, p. 133116, 2006.

[7] M. D. Fischbein and M. Drndic, "Sub-10 nm device fabrication in a transmission electron microscope," *Nano Lett.*, vol. 7, no. 5, pp. 1329–1337, 2007.

[8] M. A. Reed, C. Zhou, C. J. Muller, T. P. Burgin, and J. M. Tour, "Conductance of a molecular junction," *Science*, vol. 278, p. 252, 1997.

[9] E. P. D. Poorterea, H. L. Stormera, L. M. Huang, S. J. Wind, S. OBriena, M. Huanga, and J. Honea, "1- to 2-nm-wide nanogaps fabricated with single-walled carbon nanotube shadow masks," *J. Vac. Sci. Technol. B*, vol. 24, no. 6, pp. 3213–3216, 2006.

[10] G. Esen and M. S. Fuhrer, "Temperature control of electromigration to form gold nanogap junctions," *Appl. Phys. Lett.*, vol. 87, p. 263101, 2005.

[11] L. D. L. S. Valladares, L. L. Felix, A. B. Dominguez, T. Mitrelias, F. Sfigakis, S. I. Khondaker, C. H. W. Barnes, and Y. Majima, "Controlled electroplating and electromigration in nickel electrodes for nanogap formation," *Nanotechnology*, vol. 21, no. 44, p. 445304, 2010.

[12] T. Nagase, K. Gamo, T. Kubota, and S. Mashiko, "Direct fabrication of nano-gap electrodes by focused ion beam etching," *Thin Solid Films*, vol. 499, no. 1-2, pp. 279–284, 2006.

[13] S. M. Dirk, S. W. Howell, S. Zmuda, K. Childs, M. Blain, R. J. Simonson, and D. R. Wheeler, "Novel one-dimensional nanogap created with standard optical lithography and evaporation procedures," *Nanotechnology*, vol. 16, no. 10, p. 1983, 2005.

[14] V. Milanovic, L. Doherty, D. Teasdale, C. Zhang, S. Parsa, V. Nguyen, M. Last, and K. Pister, "Deep reactive ion etching for lateral field emission devices," *Electron Device Letters, IEEE*, vol. 21, no. 6, pp. 271 – 273, 2000.

[15] M. Mita, H. Kawara, H. Toshiyoshi, J. Endo, and H. Fujita, "Bulk micromachined tunneling tips integrated with positioning actuators," *Microelectromechanical Systems, Journal of*, vol. 14, no. 1, pp. 23–28, 2005.

[16] R. D. Grober, R. J. Schoelkopf, and D. E. Prober, "Optical antenna: Towards a unity efficiency near-field optical probe," *Appl. Phys. Lett.*, vol. 70, pp. 1354 – 1356, 1997.